GEOPHYSICAL RESEARCH LETTERS, VOL. 13, NO. 4, PAGES 303-306, APRIL 1986

ON THE INFLUX OF SMALL COMETS INTO THE EARTH'S UPPER ATMOSPHERE
I. OBSERVATIONS

L. A. Frank, J. B. Sigwarth and J. D. Craven

Department of Physics and Astronomy, The University of Iowa, Iowa City, Iowa 52242

Abstract. Images of the earth's dayglow emissions at ultraviolet wavelengths, primarily those of atomic oxygen at 130.4 nm, reveal regions of transient intensity decreases to ~ 5% to 20% of surrounding values over areas estimated to be ~ 2,000 km^2. The duration of these transient decreases in intensities is ~ several minutes. Approximately 10 of these events occur each minute in the dayside upper atmosphere. The diurnal variation of the rate of occurrence is qualitatively similar to that for radar meteors.

Introduction

The high-altitude, polar-orbiting satellite Dynamics Explorer 1 is instrumented with three imaging photometers for global surveys of the earth's auroral emissions, columnar ozone distributions and geocorona. One of these imaging photometers is capable of viewing the atmospheric dayglow primarily in the atomic oxygen (OI) emissions at 130.4 nm. Examination of these images reveals the appearance of large, transient decreases in dayglow intensities over areas of the order of several tens of kilometers in diameter. These regions appear as dark spots, or 'holes', in the otherwise generally uniform dayglow intensities. In excess of 10,000 images are being used currently in the interpretation of the source of these atmospheric holes. There are no previously published reports of this phenomenon with the exception of several oral presentations by this research group.

Observations

The earth-satellite Dynamics Explorer 1 is positioned in a polar eccentric orbit with initial perigee and apogee altitudes of 570 km and 3.65 earth radii, respectively, at launch on August 3, 1981. The precession of the line of apsides is 0.328 degree/day and provides the opportunity to globally image the earth from apogee over a wide range of points of view from over the poles and equator and spanning all local times during the past four years. The portion of the imaging instrumentation of direct relevance here is the spin-scan photometer for ultraviolet emissions, in particular when the filters passing primarily the atomic oxygen triplet emissions at 130.4 nm are employed. The filters are coated with an aluminum flashing in order to adequately suppress the sensor's responses to intense long-wavelength radiation at $\gtrsim$ 200 nm when viewing the dayside of the earth. A photomultiplier tube with a MgF_2 window and a CsI photocathode is employed as the sensor. The primary optical system is off-axis catoptric with a scanning mirror which, together with the rotation of the spacecraft about its spin axis, is used to gain the two-dimensional array of pixels comprising an image. The angular diameter of the full field-of-view corresponding to a single pixel is 0.29°. Images with angular dimensions of 30° × 120° are usually telemetered from the spacecraft. A field-of-view of 30° is sufficient to image the entire face of the earth from apogee. One image is typically obtained every 12 minutes. A discussion of the imaging instrumentation is given by Frank et al. (1981).

An image of the atmospheric dayglow at ultraviolet wavelengths is shown on the front cover (this issue). The image is false-color coded such that highest intensities are yellow, lower intensities are red and the intensities lower than that for the threshold for processing of this image are black. Interpolation between pixels is used in the image processing. The ring of emissions at the top of the image is the northern auroral oval. Several dark spots, or 'atmospheric holes', are seen in the dayglow emissions, one

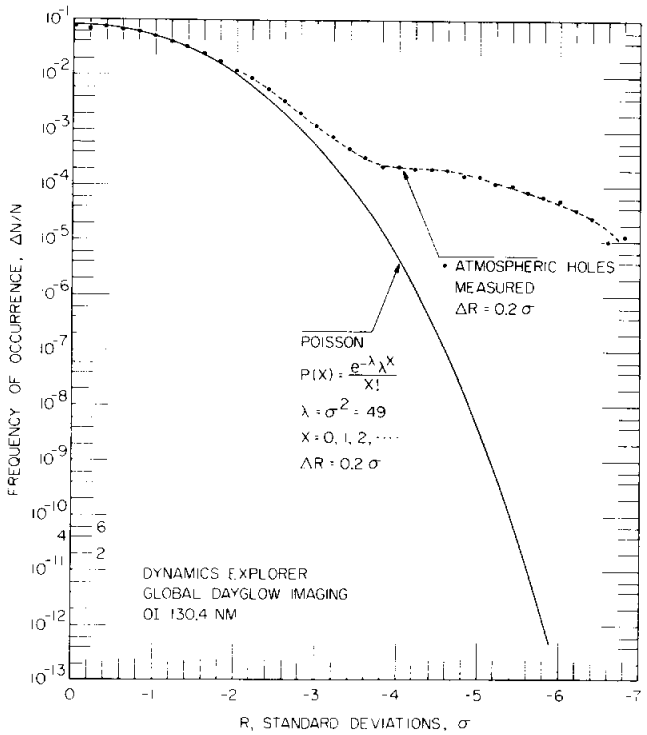

Figure 1. Comparison of the distribution of approximately 1.3 × 10^6 samples (pixels) of dayglow intensities at OI 130.4 nm with the expectations for a Poisson distribution with mean rate of 49 counts/pixel. An atmospheric hole is identified with any pixel for which R $\leq$ -4.3σ.

Paper number 6L6046.
0094-8276/86/006L-6046$03.00

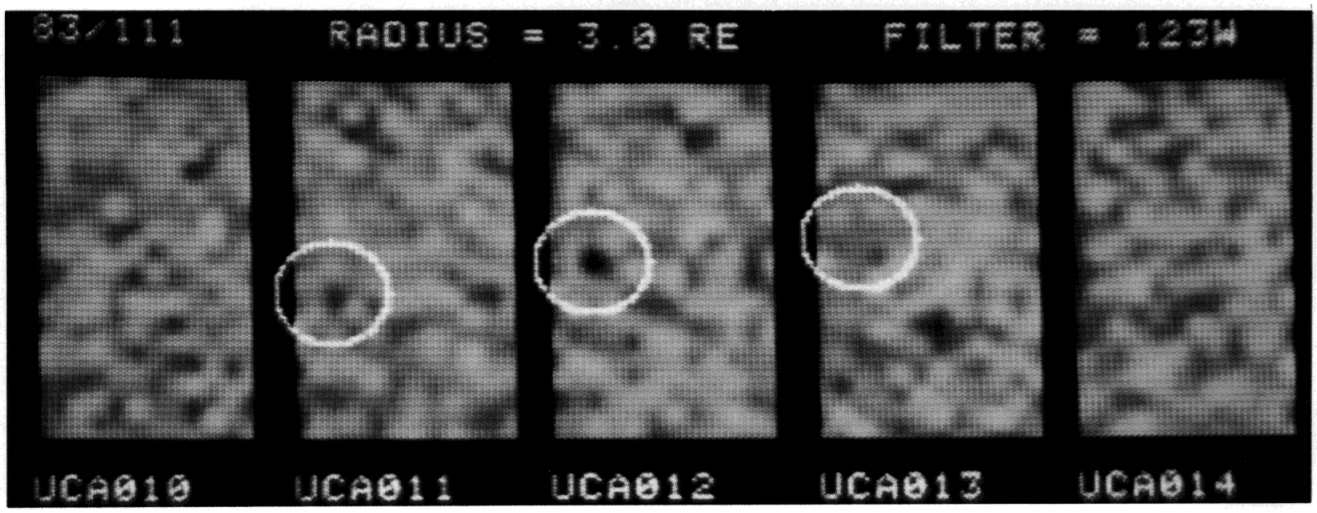

Figure 2. Sequence of images of an atmospheric hole. The central vertical scan lines of consecutive frames are separated in time by 72 seconds and scan lines are telemetered from right-to-left and left-to-right sequentially for the frames. The positions of the atmospheric hole are circled. The hole in the center frame is observed at 0642 UT on April 21, 1983 from an altitude of 12,800 km.

of which is shown in expanded view in the inset. The diameter of this region of greatly diminished intensities is ~ 150 km, and is larger than the typical hole dimension. The filter used to obtain this image excludes hydrogen Lyman α, but is sufficiently wide to include Lyman-Birge-Hopfield (LBH) emissions of molecular nitrogen, as well as the OI emissions at 130.4 and 135.6 nm. For the dayglow the intensities at OI 130.4 nm dominate the responses of the photometer. The upper atmosphere is optically deep at this latter wavelength. These oxygen emissions as viewed from the spacecraft position are due to photoelectron impact excitation and resonantly scattered solar radiation (Meier and Lee, 1982).

Considerable scrutiny of the measurements is used to demonstrate that these atmospheric holes are not due to telemetry noise or other spurious effects. Typical responses of the imaging photometer are ~ 50 counts/pixel for the dayglow intensities in regions adjacent to the atmospheric hole and are ~ 10 counts/pixel when viewing directly into the atmospheric hole. Atmospheric holes can be identified also in the weaker N_2 LBH dayglow. In addition, for the larger atmospheric holes the large decrease in dayglow intensities is seen in two adjacent lines of pixels in the images. Such samples are separated by 6 seconds. Occasionally a larger atmospheric hole can be identified in two consecutive full image frames taken at 12-minute resolution, although the typical duration of a single event appears to be $\lesssim$ 3 minutes. Such time resolution is possible since the scanning mirror successively scans from left-to-right, right-to-left and alternately favors one side of the image. In order to better observe the temporal evolution of the dayglow intensities, the imaging photometer is employed in a mode with reduced field-of-view, and hence increased temporal resolution, at the lower orbital altitudes. These observations are discussed below. Finally the diurnal variation of the frequency of these atmospheric holes is compared to that of meteors incident on the dayside of the earth (Sigwarth et al., 1985).

The results of a test of the counting statistics are shown in Figure 1. A total of $N = 1.3 \times 10^6$ samples (pixels) is used to determine their

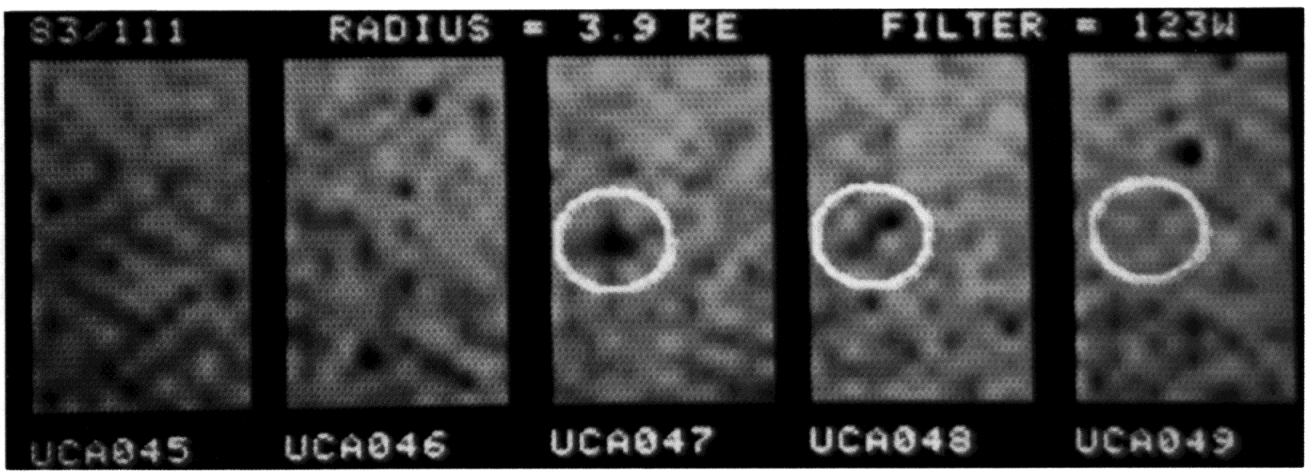

Figure 3. Continuation of Figure 2 for an atmospheric hole observed at 0726 UT on April 21, 1983 from an altitude of 18,500 km.

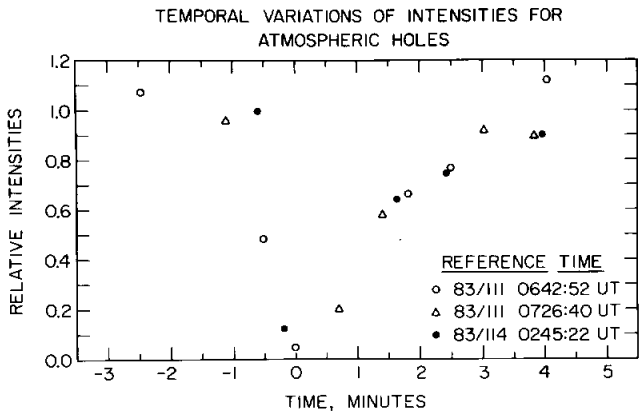

Figure 4. Intensities for the centers of three atmospheric holes relative to surrounding dayglow intensities as a function of elapsed time. These three events are superposed by matching relative intensities during recovery of dayglow intensities.

distribution as a function of the number of standard deviations, R, from a running mean of six samples. One standard deviation is σ. These six samples are the three consecutive samples each prior to and following the sample for which R is computed. The frequency of occurrence, $\Delta N/N$, in bins $\Delta R = 0.2$ as a function of R is given in Figure 1. A Poisson distribution for a mean count rate of 49 counts per pixel is included for comparison. Deviations from Poisson statistics are noticeable at $R \leq -2\sigma$ and large at $\leq -3\sigma$, A conservative value of $R \leq -4.3\sigma$ is used for positive identification of an atmospheric hole. For $R = -4.3$ ($\pm$ 0.1) the probability of observing one atmospheric hole due to counting statistics is $\sim 1.2 \times 10^{-6}$, or once in $\sim$ 400 images. This rate is a factor of $\sim 3 \times 10^{-3}$ less than the observed rate. For smaller values of R this factor rapidly decreases (see Figure 1). The larger atmospheric hole shown in the cover figure comprises two adjacent pixels with $R = -5.5\sigma$ and -5.6σ, respectively. If these responses are due to counting statistics one such event with $R \leq -4.3\sigma$ should occur in 3×10^3 years of continuous imaging, and with $R \leq -5.5\sigma$ in $\sim 10^{12}$ years. The observed occurrence rate for these larger atmospheric holes with $R \leq -4.3\sigma$ is one event every several hours.

The error rate for telemetry transmission is established by monitoring fixed bit patterns and the highest order bit from the count registers in the instrument. Dayglow intensities are insufficient to fill the registers such that this latter bit changes state. The corresponding error rate is $\sim 2 \times 10^{-6}$. Because our identification of an atmospheric hole is $R \leq -4.3\sigma$, only an error in the most significant bit is identified as an atmospheric hole. Thus an atmospheric hole due to telemetry noise is expected once in $\sim$ 200 image frames. The observed rate is a factor $\sim 10^3$ greater than that due to telemetry noise. A large atmospheric hole such as that shown in the inset of the cover figure is expected once every 1200 years of continuous imaging if the source is telemetry noise, or a factor of $\sim 3 \times 10^{-7}$ less than the observed rate. Clearly the atmospheric holes are not due to telemetry noise or counting statistics.

The sensor responses are sampled sequentially by two complete sets of count registers that are each serviced by one spacecraft telemetry word. Hence adjacent pixels in a given scan line of an image are provided by two independent sets of digital electronics. Atmospheric holes are recorded in the samples from both registers, thereby eliminating the possibility of a subtle malfunction of a single count register.

Two series of images of these transient, severe decreases in dayglow intensities with greater temporal and spatial resolutions are shown in Figures 2 and 3, respectively. Frame temporal resolution is 72 seconds for both series of observations. The spatial resolutions for the center frames for Figures 2 and 3 are 64 and 93 km, respectively, at an altitude of 200 km above the earth's surface. The positions of the atmospheric holes are centered within the circles. The center of the circle for a given image series is set at the position of the maximum decrease and then computed with knowledge of the spacecraft orbital motion and the assumption of atmospheric corotation for the remaining frames. A few other atmospheric holes can also be seen in the images. The generally mottled appearance of the upper atmosphere is primarily due to counting statistics for the pixels. The brightnesses at the centers of the atmospheric holes relative to those of adjacent regions for three such series of observations as a function of time are summarized in Figure 4. The relative times for these three individual observations are determined by matching the relative brightnesses during recovery, i.e., at 1.5 to 3 minutes. Times for observations of dimmest dayglow are also given in Figure 4. Note that the maximum decreases in intensities are to

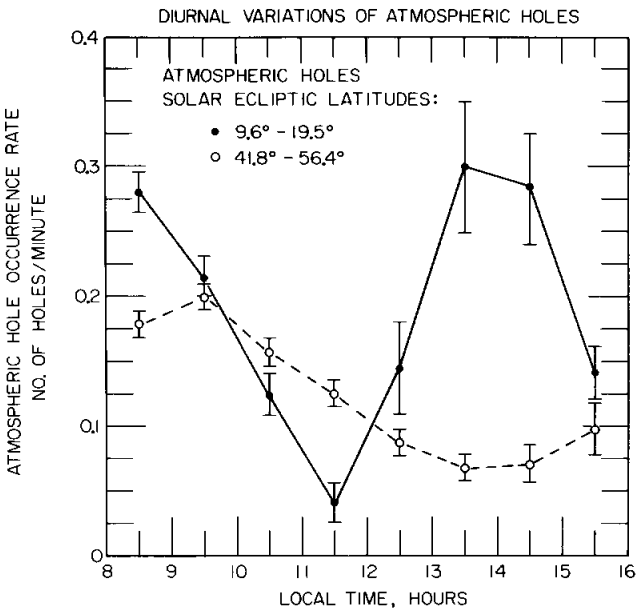

Figure 5. Diurnal variations of the occurrence rate of atmospheric holes for two latitude zones. The occurrence rate is given for an area of 1.8×10^6 km^2. Approximately 1,800 individual sightings of atmospheric holes are used in the determination of the diurnal variations shown in this figure.

$\lesssim$ 20%, and in one case to ~ 5% of the surrounding dayglow intensities. During the initial decrease in intensities, dimensions less than the spatial resolution of a pixel are consistent with the measurements.

Detection of these atmospheric holes at altitudes above the exobase is of considerable relevance to the identification of their origins. In order to observe atmospheric holes above the earth's limb, scattered solar Lyα emissions from atomic hydrogen must be used for backlighting. An appropriate altitude for usable Lyα intensities, and with sufficiently low H densities to allow a reasonable viewing distance into the geocorona, must be selected. Such observations at altitudes of ~ 3,000 km reveal some sightings of atmospheric holes at positions just above the earth's limb. The frequency of occurrence of atmospheric holes with large intensity decreases on the earth's disk is considerably lesser than that observed in the emissions of OI, presumably due to the scattering of Lyα by the H atoms along the line of sight. The detection of atmospheric holes positioned above the exobase supports identification with an extraterrestrial origin.

The diurnal variations of the occurrence rate of atmospheric holes are shown in Figure 5 for two earth-centered, solar-ecliptic latitude zones in the sunlit atmosphere, 9.6° to 19.5° and 41.8° to 56.4°. The occurrence rate is given in units of events per minute for an area of 1.8×10^6 km^2. The area bins are bounded by 15° in solar ecliptic longitude, or 1 hour in local time. At low latitudes the occurrence rate exhibits a maximum at ~ 14 hours local time that is not found at mid-latitudes. At local times ~ 8 and 16 hours the apparent rates of atmospheric holes may decline artificially due to the rapidly decreasing dayglow intensities near the terminator. The diurnal variations of atmospheric holes displayed in Figure 5 are qualitatively similar to those for radar meteor rates at Waltair, 17.7° N geographic, (Devara, 1981) and Ottawa, 45.5° N (McKinley, 1961), respectively. A maximum in radar meteor rates occurs in the early-morning sector for both latitudes. The overall character of the diurnal variations for atmospheric hole and radar meteor rates is in general agreement with that expected for a distribution of objects in predominantly direct elliptical orbits around the sun (Weiss, 1957; Vogan and Campbell, 1957).

Discussion

Large, transient decreases of dayglow intensities in the emissions of atomic oxygen at 130.4 nm are revealed in images of the earth's upper atmosphere as taken with the high-altitude satellite Dynamics Explorer 1. In addition these decreases in dayglow intensities are observed in the LBH bands of N_2 at ~ 140 to 170 nm and in the geocoronal Lyα emissions at 121.6 nm. These atmospheric holes appear initially as severe decreases of dayglow intensities by factors of 5 to 20 less than the values in surrounding regions with recovery to typical intensities within ~ 3 minutes. The area of an individual atmospheric hole is estimated to be approximately 2,000 km^2. However, this estimate for the average area of an atmospheric hole is considered accurate to a factor of ~ 3 since this phenomenon is observed near the angular resolution of the instrument. Approximately 30,000 atmospheric holes are identified in the images at this date during an observing period of ~ 2,000 hours spanning the period of late-1981 through early-1985. The average occurrence rate is approximately 10 atmospheric holes per minute in the dayside upper atmosphere. This rate corresponds to one impact on a 1-km^2 area of the upper atmosphere once each 50 years.

The diurnal variations of the rate of atmospheric holes are qualitatively similar to those for radar meteors. Thus there is evidence that the source of the atmospheric holes is extraterrestrial. The globally averaged occurrence rate of atmospheric holes, ~ 10^{-15}/m^2-sec, is similar to that for meteors with masses ~ 1 to 10 gm as given by Nilsson and Southworth (1967).

Acknowledgements. This research was supported in part by NASA under grants NAG5-483 and NGL-16-001-002 and by ONR under grant N00014-85-K-0404.

References

Devara, P.C.S., M. I. Ahmed, M. S. Rao and B. R. Rao, Meteor wind radar studies at Waltair, Ind. J. Radio Space Phys., 10, 228, 1981.

Frank, L. A., J. D. Craven, K. L. Ackerson, M. R. English, R. H. Eather and R. L. Carovillano, Global auroral imaging instrumentation for the Dynamics Explorer mission, Space Sci. Instr., 5, 369, 1981.

Frank, L. A., J. B. Sigwarth and J. D. Craven, On the influx of small comets into the earth's upper atmosphere, II. Interpretation, Geophys. Res. Lett., (this issue), 1986b.

McKinley, D. W. R., Meteor Science and Engineering, McGraw-Hill, New York, p. 113, 1961.

Meier, R. R. and J. S. Lee, An analysis of the OI 1304 Å dayglow using a Monte Carlo resonant scattering model with partial frequency redistribution, Planet. Space Sci., 30, 439, 1982.

Nilsson, C. S. and R. B. Southworth, The flux of meteors and meteoroids in the neighborhood of the earth, Smithson. Astrophys. Observ. Spec. Rep. 263, Cambridge, Mass., 1967.

Sigwarth, J. B., L. A. Frank and J. D. Craven, Latitudinal and longitudinal distribution of atmospheric holes associated with meteors, EOS Trans., 66, 1005, 1985.

Vogan, E. L., and L. L. Campbell, Meteor signal rates observed in forward-scatter, Canad. J. Phys., 35, 1176, 1957.

Weiss, A. A., The distribution of the orbits of sporadic meteors, Aust. J. Phys., 10, 77, 1957.

(Received February 6, 1986;
revised March 6, 1986;
accepted March 7, 1986.)